Raindrop Size Distribution under Drop Break-up: Implications for GPM DPR Algorithm

Leo Pio D'Adderio[1], Federico Porcù[1] and Ali Tokay[2]

[1]*Univ.of Ferrara, Dep. of Physics ans Earth Science, 44122 Ferrara*
[2]*JCET-University of Maryland Baltimore County and NASA-Goddard Space Flight Center, 20770 Greenbelt*

Leo Pio D'Adderio

1 Introduction

The Drop Size Distribution (DSD) is a relevant characteristic of precipitation and it has been intensively studied since the early days of cloud physics in natural rain (Marshall and Palmer, 1948) and in laboratory experiments (Mc Taggart-Cowan and List, 1975). The collisional break-up is one of the main mechanisms that determines the DSD shape in natural rain. In particular, when a large and a smaller drop collide if their Collisional Kinetic Energy (CKE) is not dissipated by viscous motion of water molecules inside the coalescing drops, the drops break in smaller fragments. First laboratory studies on collisional break-up were made by Mc Taggart-Cowan and List (1975) setting up an aerodynamic drop accelerator to study collisions between five pairs of drops at terminal speed. With a similar equipment, Low and List (1982a, 1982b) and List et al. (2009) increased the spectrum of drop sizes in colliding pairs and found a 3-peaks equilibrium DSD. Mc Farquhar (2004) proposed a new break-up parameterization ensuring mass conservation and estimating the uncertainties. A box model was used to derive the equilibrium DSD, characterized by two peaks around 0.26 mm and 2.3 mm and a relative minimum around 1.6 mm.

Evidence of break-up influence on DSD shape up to reach the equilibrium DSD is observed in the Zawadzki and De Agostinho Antonio (1988) and Willis and Tattelman (1989) experimental measurement. A bimodal trend for high rainfall rate values are observed. More recently, Porcù et al. (2013, 2014) measured DSDs at different altitude and observed the break-up evidence with a bimodal DSD shape. They found that diameters involved are different, depending on altitude, but the CKE assumes very close values due to the effects of the reduced air density on the drops terminal velocity.

The three-parameter gamma distribution is generally used to model the DSD and has been widely used and is adopted for retrieval of DSD from spaceborne radar measurements including National Aeronautics and Space Administration (NASA) Tropical Rainfall Measuring Mission (TRMM) precipitation radar (Kozu et al. 2009) and Global Precipitation Measurement (GPM) mission dual-frequency radar (Seto et al. 2013). Willis and Tattelman (1989) fitted the experimental DSDs with gamma distribution and computed the squared error for each measured distribution over a wild range of rainfall intensity and at different location. They found that the gamma distribution is a good approximation. Cao and Zhang (2009) calculated the bias and fractional error for different moment estimators of measured and gamma modelled DSD. Their results show that generally middle-moment estimators produce lower error, except when the DSD is not well fitted by gamma distribution; in that case, the moment order depends on the considered estimator.

The main aim of this work is to set up an automatic break-up detection algorithm to be applied to experimental DSD as measured by disdrometers. The algorithm is applied to a large and heterogeneous, in terms experimental locations, disdrometric dataset to highlight the characteristics of DSD affected by break-up (equilibrium DSD). A comparison with fitted gamma distribution is made in order to understand if in these situations this parameterization can be considered the optimal choice. The behavior of some DSD parameters is also analyzed searching particular properties to be used as a discriminant to recognize the situations that support the break-up mechanism. Finally, the time series analysis is an additional indicator on which cloud structure allows the break-up formation.

2 Background and methodology

Data used for the present work were collected in six different measurement campaigns, by using two different disdrometers: Two-Dimensional Video Disdrometer (2DVD, Schönhuber et al., 1994) and Particel Size Velocity disdrometer (Parsivel^2, (Loffler-Mang, 1998). Table 1 describes in detail the characteristics of each filed campaign reporting latitude and longitude, duration and number of minutes analyzed. The IFLOODS, MC3E, IPHEX and LPVEX campaigns fall back to the GPM Ground Validation (GV) program (Matsui et al., 2013).

All data collected were analyzed to recognize break-up minutes by studying the DSD characteristics. The key feature is the 2- or 3-peak DSD shape with the presence of a relative minimum followed by a relative maximum. According to McFarquhar (2004) and Pratt and Barros (2007) the position in the DSD spectrum of relative minimum and maximum is around 1.5 and 2.5 mm respectively. Collisional break-up generally takes place when the CKE is higher than 5 μJ and it is able to modify the DSD shape when a drop at a size of around 1.5 mm diameter collides with a drop larger than 3 mm. The result of break-up situations is a depletion of drops around 1.5 mm, an increase of very small drops (size below 1 mm) and an increase of drops around 2.5-3 mm with the formation of the relative minimum and maximum.

Table 1. Field campaigns description.

Field campaign	Lat, Lon (°)	Duration	Data collected (min)
Iowa Flood Studies (IFLOODS)	42°N, 92°W	May 1st to June 15th 2013	3992
Midlatitude Continental Convective Clouds Experiment (MC3E)	36°N, 97°W	April 22nd to June 6th 2011	702
Wallops Flight Facility (Wallops)	37°N, 75°W	July 2013 to March 2014	3594
Alabama	35°N, 87°W	December 2009 to June 2010	870
Integrated Precipitation and Hydrology EXperiment (IPHEX)	35°N, 83°	May 1st to June 15th 2014	2088
Light Precipitation Validation Experiment (LPVEX)	60°N, 24°E	September 15th to December 31st 2010	120

The main objective of this work is to develop an algorithm to automatically detect break-up spectra in natural rain. The algorithm is designed to recognize break-up features in the DSD, as sketched in Figure 3, and to rank the DSD accordingly. It works through the following steps:

- the linear best fit of the considered DSD is calculated over a five DSD diameter bins, from the starting point toward larger diameters
- four different starting points are considered, from 1.0 to 1.6 mm (with steps of 0.2 mm), so that four linear relationship are calculated
- the highest slope (SL) value of the linear best fit functions obtained is considered as reference to label the DSD
- the DSDs are sorted from the lowest (negative) to the highest (positive) SL value.

The algorithm looks for the concavity change in the part of DSD spectrum between 1.0 and 2.6 mm diameter, based on the slope of the linear best fit (see Figure 3, red line), assuming that a concavity change in that part of DSD spectrum denotes the certain presence of break-up, eventually to reach equilibrium DSD.

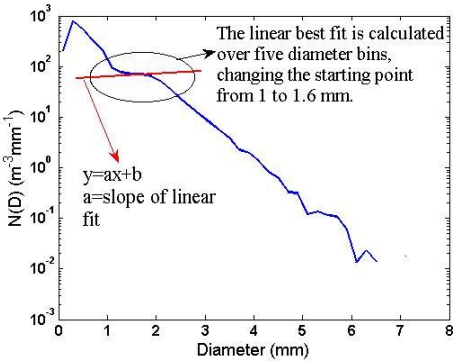

Figure 1: Example of the method application on DSD spectrum.

The data were averaged over 2 minutes to have a more stable signal and a threshold of 5 mmh^{-1} was considered to eliminate the stratiform event, assuming break-up takes place especially during convective precipitation. The main discussion is carried on the 2DVD data, because several instruments were installed in each considered campaign and a larger dataset is available. A short paragraph, however, describes the Parsivel[2] performances (data are available just from three of six campaigns analyzed), showing the reliability of algorithm regardless the instrument type.

3 Results and discussion

3.1 2DVD analysis

All data sorted according to the method above described, are dived in six SL classes and the mean DSD for each class is computed. Since the most part of DSDs have slope between 0 and -2, this interval was divided in four classes with steps of 0.5 (classes from 2 to 5), and the remaining two classes are defined with SL>0 (class 1) and with SL< -2 (class 6). Figure 2 shows the mean DSD, normalized with the rainfall rate, for each class for the different datasets, highlighting the marked variation of DSD shapes as function of SL classes. The DSDs with positive SL have good agreement with those obtained by different models in presence of break-up and defined as equilibrium DSD (McFarquhar, 2004; Pratt and Barros, 2007): accordingly, we label the DSD belonging to class 1 as equilibrium DSD. The class 2, with -0.5<SL<0 marks the transition from situations where mature break-up is present (class 1) to situation where break-up is yet present but it is not able to modify the DSD shape considerably. Considering lower SL values, the DSD does not represent any more mature break-up situations. In this sense we

can refer to class 2 as transition class: the transition becomes complete with class 3 where break-up, even if occasionally occur, has not effects on the DSD shape. The classes from 3 to 6 show a DSD shape that can be fully approximated by a gamma distribution with variable parameters depending on the class considered.

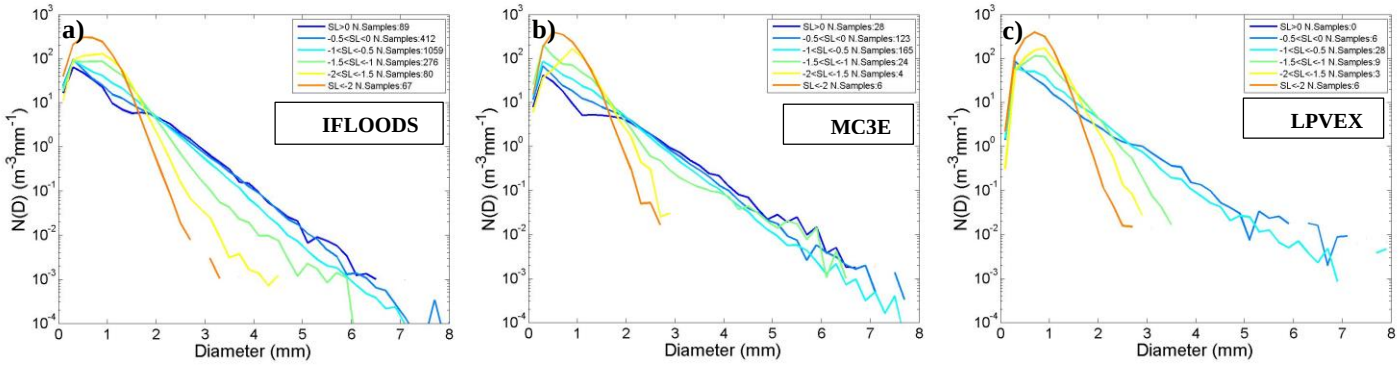

Figure 2: Mean DSD for each class for three different measurement campaigns.

The DSDs have positive SL in a low percentage of cases marking the fact that equilibrium DSD is rarely reached in natural rain. The percentage value depends on the season also: the maximum value (8%) is obtained for MC3E campaign carried on during the spring season, but also IPHEX records a high value (5.8%). Wallops percentage for class 1 (2.4%) and 2 (11.3%) are lower because the most part of data are collected in fall and winter. The low latitude of Wallops also enables to have rain intensities exceeding the threshold used here, but that are due to stratiform systems in which break-up is less frequent. In these situations, SL assumes negative values and this contribute to decrease the percentage for classes 1 and 2. Considering the classes 1 and 2 together, the percentage reaches significant values, up to about 45% for MC3E campaign. This remarks that break-up is more frequent during convective episodes, but only in few cases is able to modify the DSD up to reach the equilibrium DSD. High percentage values are obtained both for class 1 and 2 for IPHEX and IFLOODS campaigns also. LPVEX dataset records the lowest values of occurrence for class 1 (0%) and 2 (11.5%) and it is a very significant dataset. First of all the sample size is small, this is indicative of the fact that convective events at high latitude are not so common. Furthermore, the high latitude is a factor that inhibits the convective development, causing the absence of DSDs in the class with positive SL. This evidences that break-up takes place exclusively during convective rain and that it is fundamental to reach the equilibrium DSD.

3.2 Parsivel^2 analysis.

The same analysis has been carried on using data from Parsivel^2 data for IFLOODS, IPHEX and Wallops campaigns. The results (not shown here) are in good agreement with what found for 2DVD data: class 1 shows the DSD equilibrium, more markedly for IFLOODS and IPHEX data, and class 2 can be considered as the transition class according to the definition given above. The diameters interested by the break-up feature are the same the 2DVD. This dispels all doubt on other possible explanations about the characteristic evidenced in class 1 (i.e. instrument systematic bias and specificity). The results differ from 2DVD data if the percentage of occurrence in each SL class is considered and are rather different with respect 2DVD for class 1 and 2, while there is a better agreement for class from 3 to 6. This is mainly due to the larger and variable size of DSD bins. This instrument characteristic does not allow recognizing the most part of break-up cases. Furthermore, this evidences as the diameters involved in break-up process have well defined sizes.

3.3 Gamma distribution and experimental DSD.

The three parameters gamma distribution (Ulbrich, 1985) is widely used to parameterize the DSD and to retrieve the DSD parameters from radar/satellite measurements and in cloud modeling. The explicit expression of a DSD assumed to be a gamma distribution is:

$$N(D) = N_0 D^{\mu} e^{-\lambda D} \qquad (1.1)$$

where N_0 (mm^{-1}m^{-3}) is the intercept parameter, μ is the shape parameter that can assume both positive and negative values, and λ (mm^{-1}) is the slope parameter and assumes positive values only. The method of moments of order 3, 4 and 6 is applied to calculate the gamma distribution. The Pearson correlation coefficient between the experimental DSDs and the corresponding estimated gamma distribution is calculated, both on the whole DSD spectrum and in the 1.0-2.6 mm interval, in order to understand how the gamma fits the DSD in presence of break-up. Figure 3 shows the correlation coefficient between the experimental DSDs and the estimated gamma distributions for IFLOODS dataset. Figure 3a is referred to the correlation considering the whole DSD spectrum, while figure 3b is referred to the 1.0-2.6 mm interval only. The colors are in according with the SL classes.

The results show a clear trend moving from class 6 to class 1. The correlation is relatively higher for SL classes from 3 to 6, above 0.8 and 0.9 considering the whole spectrum and the 1.0-2.6 mm interval respectively. Class 2 marks the transition to low correlation coefficient values, which with some exceptions, are a characteristic of class 1. This clearly evidences that

gamma distribution is not a good approximation for break-up situations. Probably another distribution or a different gamma form can be more suitable to describe the break-up phenomenon.

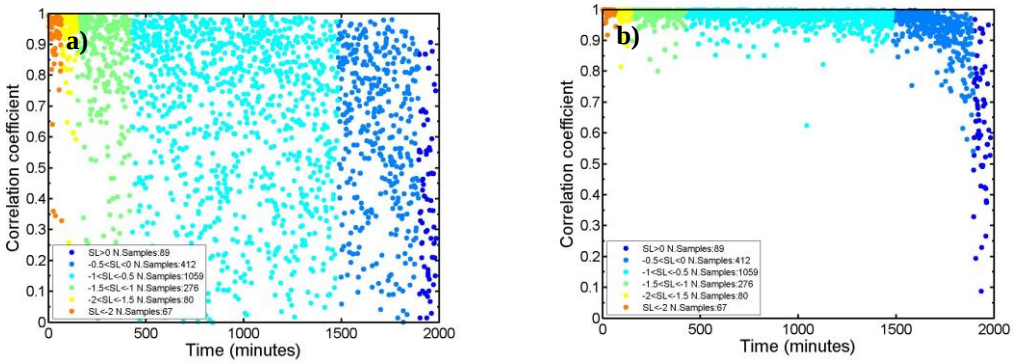

Figure 3: correlation coefficient between experimental DSDs and corresponding estimated gamma distribution as function of SL class for IFLOODS dataset, considering a) the whole DSD spectrum and b) only the 1.0-2.6 mm interval.

3.4 DSD parameters analysis.

The study of some parameters that characterize the DSD can be helpful to understand which situations can support the break-up development. Three DSD parameters (rainfall rate (RR), reflectivity (Z) and maximum diameter (D_{max})) have been studied as function of SL class. Figure 4 shows the trend of the analyzed parameters as function of SL for IPHEX dataset. All parameters, except that rainfall rate, show a clear trend with a defined different threshold moving from class 1 to 6. The results show that break-up takes place when big drops are present in the DSD (Figure 4c): this is in agreement with the fact that the CKE of two colliding drops has to be high enough to have break-up. The study of reflectivity can have additional implications because of its immediate application on radar measurement: break-up takes place for high values of reflectivity, generally above 35 dBZ (Figure 4b). A sort of trend can be noted also for rainfall rate (moving from class 6 to 1, rainfall rate generally increases, Figure 4a), but unlike the others parameter is not possible to define a threshold value, above the 5 mmh^{-1}, to establish when break-up is present. This is probably due to the lighter weight that DSD shape has on rainfall rate calculation with respect to reflectivity, depending on moment of order 3.67 and 6 respectively; this means that different DSD can give same (or similar) rainfall rate values, but surely give different reflectivity values.

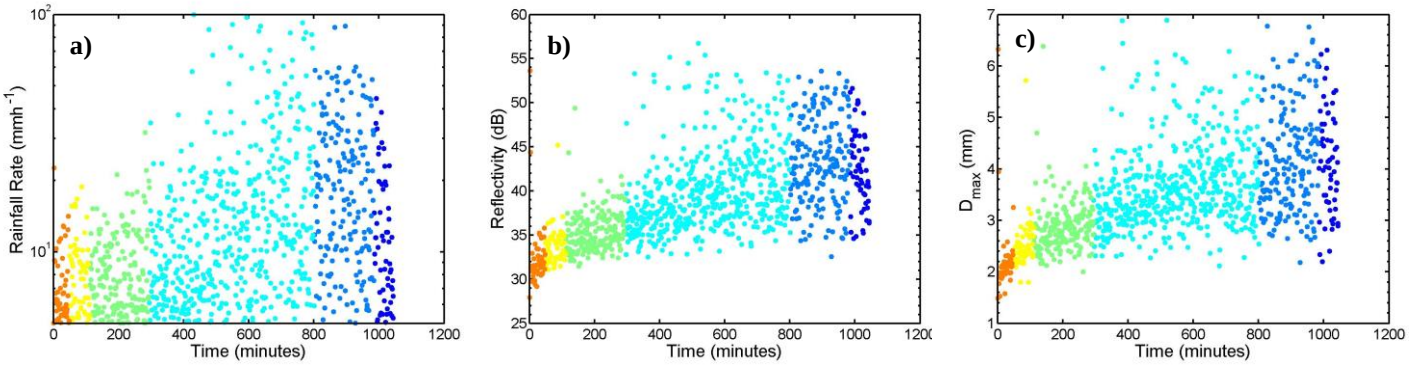

Figure 4: DSD parameters as function of SL class for IPHEX dataset. a) rainfall rate, b) reflectivity and c) maximum diameter.

3.5 Time series analysis.

The time series analysis of rainfall rate and SL values can give important indications on the cloud structure favorable to the

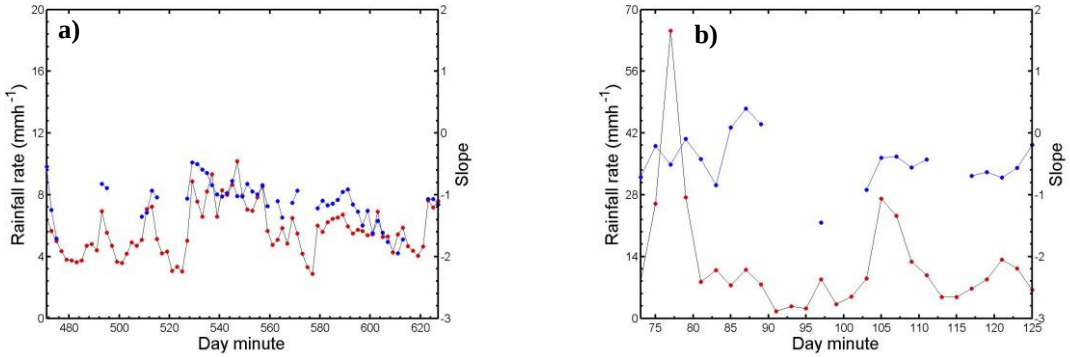

Figure 5: Time series analysis for rainfall rate and SL for a) February 13, 2014 event and b) September 13, 2013 from Wallops dataset

break-up. Figures 5a and 5b report the time series analysis for two different events collected during Wallops campaign, February 13, 2014 and September 13, 2013 respectively. There is a strong difference for both rainfall rate and SL parameter trend comparing the two events. Figure 5a shows a continuous and constant trend for rainfall rate values that never excides the 10 mmh^{-1}. A corresponding constant trend is shown by the SL time series with always negative values ranging from -0.6 to -2. A very different situation is shown in figure 5b where an irregular rainfall rate trend characterizes this event. The rain intensity jumps from low to high values, about 70 mmh^{-1}, during the whole event duration and, simultaneously, the SL jumps from negative to positive values marking the break-up presence. The characteristics evidenced by the time series in figure 5b denotes that convective cloud structure supports the break-up development compared with a stratiform cloud structure.

4 Conclusions

An algorithm has been developed to automatically detect break-up features in the DSD spectrum, using data from an unprecedented dataset. Results show that the DSDs of class 1 (SL>0) are in excellent agreement with what different model and laboratory studies describe as equilibrium DSD, characterized by 2-peaks shape. Moreover, the gamma distribution, widely used to parameterize the DSD, does not fit well the DSD when break-up is present. The study of DSD parameters as function of SL class shows that, for some parameters, a threshold can be set to discriminate the break-up situations. The time series analysis is an additional indicator about which cloud structure supports the break-up development.

Acknowledgement

It was possible to carry out this work thanks to the support of the "Fondo di Ateneo" of University of Ferrara, IUSS – Ferrara 1931 and CEOP-AEGIS, an FP7 EU project (http://www.ceop-aegis.org/) coordinated by the Université de Strasbourg ((Call FP7-ENV-2007-1 Grant nr. 212921). The 2DVD and Parsivel^2 data that were used for this work were provided through NASA Wallops Flight Facility Precipitation Data Management group.

References

Cao, Q., and Zhang G. Errors in estimating raindrop size distribution parameters employing disdrometer and simulated raindrop spectra. 2009, J. Appl. Meteor. Climat, 48(3), 406-425.

Kozu, T., Iguchi T., Shimomai T. and Kashiwagi N. Raindrop Size Distribution Modeling from a Statistical Rain Parameter Relation and Its Application to the TRMM Precipitation Radar Rain Retrieval Algorithm. 2009 J. Appl. Meteor. Climatol., 48, 716–724.doi: http://dx.doi.org/10.1175/2008JAMC1998.1

List R., Nissen R. and Fung C. Effects of pressure on collision, coalescence, and breakup of raindrops. Part II: Parameterization and spectra evolution at 50 and 100 kPa. 2009, J. Atmos. Sci., 66, 2204–2215.

Löffler-Mang M. and Joss J. An optical disdrometer for measuring size and velocity of hydrometeors. 2000, J. Atmos. Ocean. Technol., 17, 130-139.

Low, T. B. and List R. Collision, coalescence and breakup of raindrops. Part I: Experimentally established coalescence efficiencies and fragment size distributions in breakup. 1982, J. Atmos. Sci., 39, 1591–1606

Marshall, J.S. and Palmer, W.M. The distribution of raindrops with size. 1948, J. Meteorol. 5, 165–166.

Matsui, T., and Coauthors GPM Satellite Simulator over Ground Validation Sites. 2013, Bull. Amer. Meteor. Soc., 94, 1653–1660.

McTaggart-Cowan, J.D. and List R. Collision and breakup of water drops at terminal velocity. 1975, J. Atmos. Sci., 32, 1401–1411.

McFarquhar G. M. A new representation of collision-induced breakup of raindrops and its implications for the shapes of raindrop size distributions. 2004, J. Atmos. Sci. 61, 777–794.

Porcù, F., D'Adderio L.P., Prodi F. and Caracciolo C. Effects of altitude on maximum raindrop size and fall velocity as limited by collisional breakup. 2013, J. Atmos. Sci., 70, 1129–1134, doi: http:10.1175/JAS-D-12-0100.1.

Porcù, F., D'Adderio L.P., Prodi F. and Caracciolo C. Rain Drop Size Distribution over the Tibetan Plateau. 2014, Atm. Res., 10.1016/j.atmosres.2014.07.005.

Pratt, O. P. and Barros A.P. A Robust Numerical Solution of the Stochastic Collection–Breakup Equation for Warm Rain. 2007, J. App. Meteor. Climatol. 46, 1480-1497.

Schönhuber, M., Urban, H.E., Baptista, J.P.V., Randeu, W.L., and Riedler, W. Measurements of precipitation characteristics by a new disdrometer. 1994, Proc. of Atm. Phy. and Dyn. in the Analysis and Prognosis of Precipitation Fields. Rome

Seto, S., Iguchi, T., and Oki, T. The basic performance of a precipitation retrieval algorithm for the global precipitation measurement mission's single/dual-frequency radar measurements. 2013, IEEE Transactions on Geoscience and Remote Sensing, 51, 5239-5251.

Ulbrich, C. W. The Effects of Drop Size Distribution Truncation on Rainfall Integral Parameters and Empirical Relations. 1985, J. Climate Appl. Meteor., 24, 580–590.

Willis P.T., and Tattelman P. Drop-Size Distributions Associated with Intense Rainfall. 1989, J. of App. Meteor., 28, 3-15.

Zawadzki I. M. and De Agostinho Antonio Equilibrium Raindrop Size Distributions in Tropical Rain. J. Atmos. Sci., 45, 3452-3459.